TECHNICAL REPORT AMR-SS-08-11

RELATING VORTICITY CONFINEMENT TO THE MENTER SHEAR STRESS TRANSPORT TURBULENCE MODEL

Milton E. Vaughn, Jr.
System Simulation and Development Directorate
Aviation and Missile Research, Development, and Engineering Center

January 2008

DESTRUCTION NOTICE

FOR CLASSIFIED DOCUMENTS, FOLLOW THE PROCEDURES IN DoD 5200.22-M, INDUSTRIAL SECURITY MANUAL, SECTION II-19 OR DoD 5200.1-R, INFORMATION SECURITY PROGRAM REGULATION, CHAPTER IX. FOR UNCLASSIFIED, LIMITED DOCUMENTS, DESTROY BY ANY METHOD THAT WILL PREVENT DISCLOSURE OF CONTENTS OR RECONSTRUCTION OF THE DOCUMENT.

DISCLAIMER

THE FINDINGS IN THIS REPORT ARE NOT TO BE CONSTRUED AS AN OFFICIAL DEPARTMENT OF THE ARMY POSITION UNLESS SO DESIGNATED BY OTHER AUTHORIZED DOCUMENTS.

TRADE NAMES

USE OF TRADE NAMES OR MANUFACTURERS IN THIS REPORT DOES NOT CONSTITUTE AN OFFICIAL ENDORSEMENT OR APPROVAL OF THE USE OF SUCH COMMERCIAL HARDWARE OR SOFTWARE.

REPORT DOCUMENTATION PAGE

Form Approved
OMB No. 074-0188

1. AGENCY USE ONLY	2. REPORT DATE	3. REPORT TYPE AND DATES COVERED
	January 2008	Final

4. TITLE AND SUBTITLE
Relating Vorticity Confinement to the Menter Shear Stress Transport Turbulence Model

5. FUNDING NUMBERS

6. AUTHOR(S)
Milton E. Vaughn, Jr.

7. PERFORMING ORGANIZATION NAME(S) AND ADDRESS(ES)
Commander, U.S. Army Research, Development, and Engineering Command
ATTN: AMSRD-AMR-SS-AT
Redstone Arsenal, AL 35898

8. PERFORMING ORGANIZATION REPORT NUMBER
TR-AMR-SS-08-11

9. SPONSORING / MONITORING AGENCY NAME(S) AND ADDRESS(ES)

10. SPONSORING / MONITORING AGENCY REPORT NUMBER

11. SUPPLEMENTARY NOTES

12a. DISTRIBUTION / AVAILABILITY STATEMENT
Approved for public release; distribution is unlimited.

12b. DISTRIBUTION CODE
A

13. ABSTRACT ***(Maximum 200 Words)***

The U.S. Army Aviation and Missile Research, Development, and Engineering Center (AMRDEC) has been applying a Government-developed, productivity-oriented, Computational Fluid Dynamics (CFD) methodology to the aerodynamic design of Army missiles. This methodology, dubbed Euler Tunnel Analysis (ETA), uses automated grid generation software and a robust Euler solver to drastically reduce the time required to set up and execute flowfield computations. In addition, it has the capability to exercise the vorticity confinement technique in the field (to preserve tip vortices) and on the body surface (to mimic viscous effects). ETA was applied to a supersonic missile configuration with a high fineness ratio body, low aspect ratio tail fins, and a deflectable nose (used for aerodynamic control). In addition, an equation was derived to relate the surface confinement coefficient to physical parameters. Computations were made with and without vorticity confinement. Afterwards comparisons were made against wind tunnel data to assess ETA's ability to produce meaningful results. It was found that the equation yielded reasonably successful values for the surface coefficient. It was also observed that the use of surface vorticity confinement improved the accuracy of normal force, pitching moment, and yawing moment calculations.

14. SUBJECT TERMS
Applied Computational Fluid Dynamics (CFD), Productivity-Oriented, Aerodynamic Design, Vorticity Confinement, Turbulence Model, Menter Shear Stress Transport (MSST)

15. NUMBER OF PAGES
26

16. PRICE CODE

17. SECURITY CLASSIFICATION OF REPORT	18. SECURITY CLASSIFICATION OF THIS PAGE	19. SECURITY CLASSIFICATION OF ABSTRACT	20. LIMITATION OF ABSTRACT
UNCLASSIFIED	UNCLASSIFIED	UNCLASSIFIED	SAR

NSN 7540-01-280-5500

Standard Form 298 (Rev. 2-89)
Prescribed by ANSI Std. Z39-18
298-102

ACKNOWLEDGEMENTS

This work was supported in part by a grant of High Performance Computer (HPC) time from the NAVal Oceanographic (NAVO) Department of Defense (DoD) HPC center on their Cray-SVI and IBM P4 computers.

TABLE OF CONTENTS

LIST OF ILLUSTRATIONS

I. INTRODUCTION

The Euler Tunnel Analysis (ETA) suite has been demonstrated to be a valuable tool in the aerodynamic design of missiles at the U.S. Army Aviation and Missile Research, Development and Engineering Center (AMRDEC) [1]. It provides a high-fidelity, complementary collaborator to quick, preliminary design methods such as Missile DATCOM [2], AP05 [3], and Missile3 [4]. And it offers a straightforward, easy-to-use alternative to the fragmented approach of employing multiple intermediate- to high-fidelity techniques (like the S/HABP [5] piecemeal method; the CMARC [6] and PANAIR [7] panel codes; the ZEUS [8] marching technique; parabolized Navier-Stokes schemes; and full-field, elliptical approaches, that is, potential flow, Euler, and Navier-Stokes Computational Fluid Dynamics (CFD) solvers) to construct the flight characteristics of a missile.

ETA does this by assembling the components needed to conduct an Euler flowfield analysis (including an automated grid generator and a robust solver) within a single framework. This substantially reduces the time and specialized knowledge required to generate grids and setup/operate the solver, resources that are often unavailable to the aerodynamic designer. In addition, the ETA solver incorporates the vorticity confinement technique [9] to conserve field vortices and mimic surface turbulence. With these attributes, ETA is capable of greater productivity, physical fidelity, and accuracy than is typical of most Euler approaches.

II. METHODOLOGY

A. Description

ETA is a suite of Government-owned, productivity-oriented, CFD software developed to facilitate aerodynamic design and analysis. As mentioned above, it contains an automated grid generator and a robust Euler solver. However, it also contains a geometry generation code, named CFDGEN, to construct configurations from a library of pre-existing models and model parts. CFDGEN does not require Computer Aided Design / Computer Aided Manufacturing (CAD/CAM) expertise so the aerodynamic designer can use it to construct body geometries without specialized training. Although straightforward to use, CFDGEN is not visually interactive and thereby cumbersome to apply. To circumvent this inconvenience, the AMRDEC often utilizes some of the less expensive commercial CAD/CAM packages to construct, convert, and repair configurations of interest.

With regards to automated grid generation, ETA exercises the cubes component of the NASA/Ames Cart3D [10] methodology developed by Aftosmis, Melton, and Berger. This technique produces an unstructured, Cartesian field grid around the body with relatively few user inputs. The time required to do so is typically less than an hour for most of the AMRDEC's cases—an attribute that saves numerous man-hours when setting up computations. In addition, ETA utilizes the Cart3D geometry import and conversion programs. Hence, it interfaces with several geometry formats. However, the NASA Langley Wireframe Geometry Standard (LaWGS) format (produced by CFDGEN) and the stereolithography (STL) solid model format (produced by many CAD/CAM packages) are the ones most often used by the AMRDEC.

The flow solver component of ETA is the NASA/Ames Topology Independent Gridding Euler Refinement (TIGER) [11] code originally developed by Melton and modified by Robinson [12,13]. It is an explicit, unstructured, hexahedral, finite-volume, Euler CFD method that employs Jameson's Runge-Kutta scheme [14] for time integration. The enhancements made by Robinson extend the code by: (1) permitting use of an algebraic enthalpy equation in lieu of the differential energy equation, (2) generalizing the Runge-Kutta integration scheme from its original four-stages to m-stages specified by the user (usually two), (3) enhancing robustness near corners and other high-gradient regions at high Mach numbers, and (4) adding the vorticity confinement technique [9] to conserve vorticity in the field and over solid bodies.

A Graphical User Interface (GUI) and several software scripts enable: (1) editing of body geometries and the deflection of control surfaces, (2) generation of the solution grid, (3) establishment of a directory structure and flow solver input files (based on Mach number, roll angle, and angle of attack), (4) creation of the required directory structures and input files, (5) submission of cases to the computational platform, (6) checking the status of each case, (7) retrieval of the results, and (8) calculation of aerodynamic coefficients from each flowfield solution for each point of interest.

B. Initial Application

ETA was initially applied to an eight-finned missile configuration (Fig. 1) that uses a bent nose to effect aerodynamic control. The baseline geometry was constructed with CFDGEN using wind tunnel model blueprints and it incorporated three-dimensional fin thickness as well as edge radius, thickness taper, and breakline sweep angles. The nose angle was then varied to create individual representations for each deflection angle.

For each bent nose geometry, the input to cubes was set to create a field grid with the upstream boundary approximately 0.19 body lengths away from the missile. The downstream boundary was 1 length away, and the side boundaries were located from 1.5 to 1.9 lengths away (Fig. 2). The flow conditions were set to freestream values on each boundary, while the minimum grid cell dimensions were set to approximately one one-thousandth (1/1000) of the body length. Six levels of refinement were also specified which resulted in grids populated with approximately one million (1,000,000) Cartesian cells. Computations were then performed in strictly Euler mode (without vorticity confinement) for a Mach number of 3.0; roll angles of 0, 45, and 90 degrees; and angles of attack from –10 to +10 degrees.

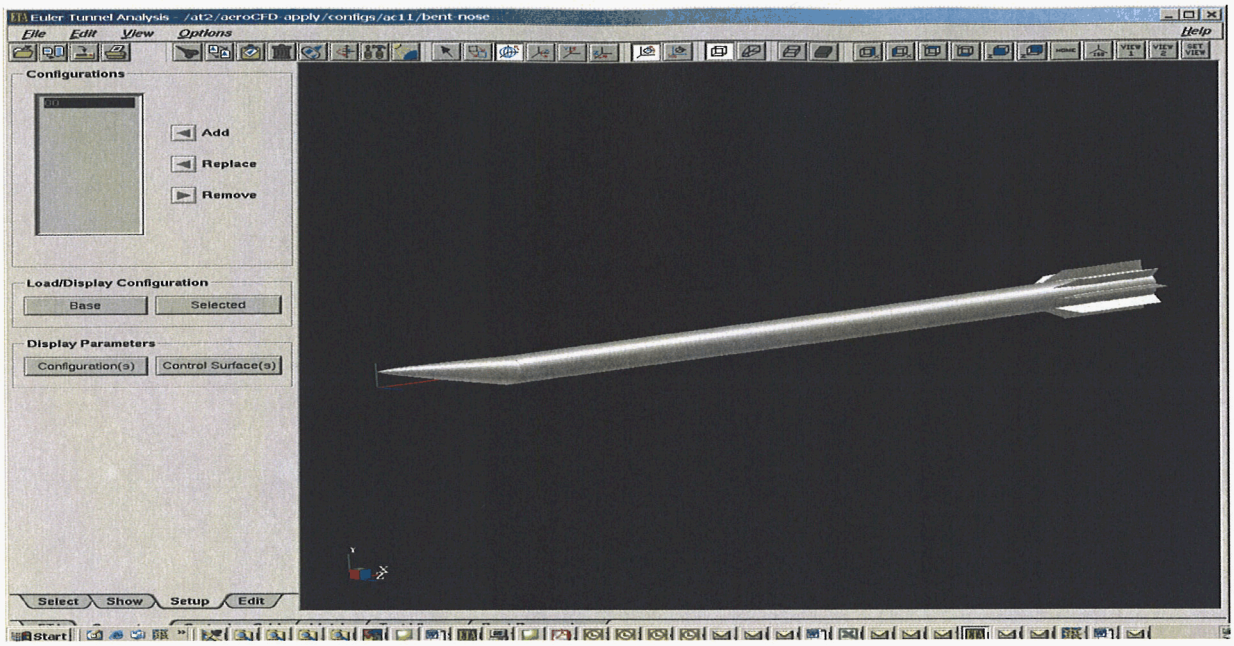

Figure 1. Bent-Nose Missile - Delta 8 Degree Nose

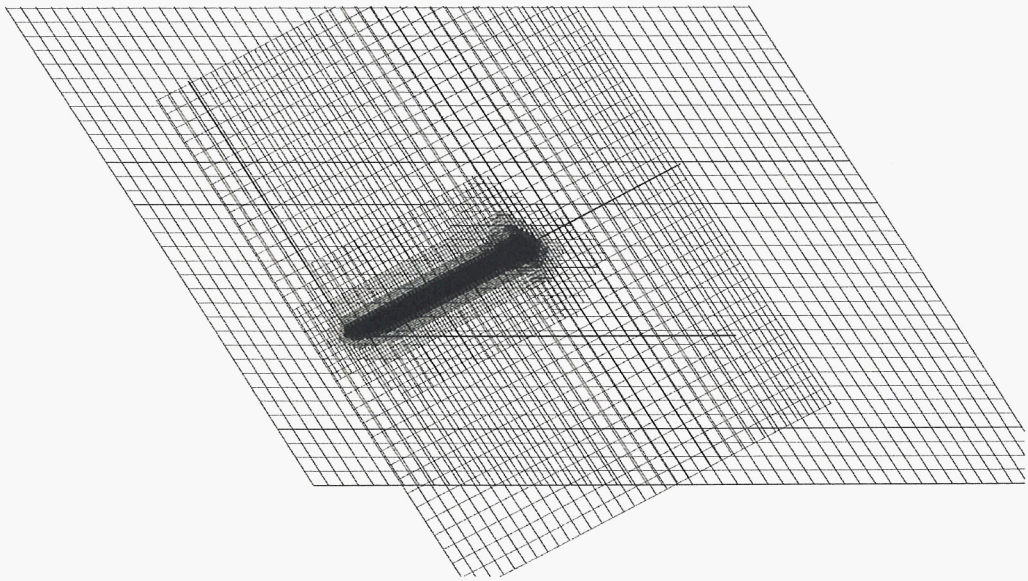

Figure 2. Typical Grid for Bent-Nose Missile Bodies

C. Surface Confinement Coefficient

The implementation of vorticity confinement in ETA is described in Reference 13 which states, "The essential feature of compressible vorticity confinement involves the addition of an anti-diffusive term to the momentum equations, proportional to the local vorticity magnitude and in a direction opposed to the numerical diffusion of vorticity ..." This term takes different forms for field and surface corrections, but each approach requires a user-specified input constant to establish the degree of correction that will be applied. Experience has demonstrated that the default field confinement coefficient in ETA (established by Robinson) appears to be adequate for the most part. However, the surface confinement coefficient is more problematic since the corrections it governs are directly related to viscous flow phenomena (usually turbulent) at and near the wall for both attached and separated flows. Since there are currently no general, physically-based guidelines for determining appropriate values of this constant, an attempt was made to rectify this situation for the problem at hand.

If the Euler equations with surface confinement terms are equated to the Favre-averaged form of the Navier-Stokes equations, a relationship can be established between the confinement parameter and the viscous terms. Then the approach used in developing the compressible Mentor Shear Stress Transport (SST) turbulence model [17, 18] is followed. In this method, the turbulence production term is presumed to be identical for both compressible and incompressible forms of the Navier-Stokes equations. Since the flow adjacent to the wall is very likely to be incompressible in the laminar sublayer, the incompressible form of the equations is used. By assuming turbulence production to be homogeneous and turbulent viscosity to be spatially constant for the local flow, it is possible to express the production in terms of vorticity. Since the laminar and turbulent viscous terms of the Navier-Stokes equations have the same form (due to the Boussinesq assumption) the laminar components of the equations can likewise be articulated in terms of vorticity.

The net result is (utilizing Robinson's notation in Reference 13, Anderson et. al.'s notation in Reference 19, and Hinze's notation in Reference 20)

$$\varepsilon_S \rho h^2 \left(-\vec{\nabla}\left|\vec{\omega}\right|\times\vec{\omega}\right) = -\frac{\mu}{2}\vec{\nabla}\left(\frac{\left|\vec{\omega}^2\right|}{\left(\frac{\partial u_i}{\partial x_j}\right)}\right) \tag{1}$$

where ε_S is the surface confinement coefficient, ρ is the fluid density, h is the representative dimension of the computational cell, ω is the local vorticity, $\mu = \mu_{laminar} + \mu_{turbulent}$ (i.e., the sum of the laminar and turbulent eddy viscosities), x_j is the Cartesian coordinate in the j direction, and u_i is the local velocity component in the i direction. By performing an order of magnitude analysis on the various terms this equation simplifies to

$$\varepsilon_S = \sqrt{2}\frac{\mu}{\rho u h} \tag{2}$$

which relates the surface confinement coefficient to a combined laminar/turbulent form of Reynolds number.

From Wilcox [21] the "outer" part of the Cebeci-Smith "mixing length" turbulence model is shown to be given by

$$\mu_{turbulent} = 0.0168\,\mu_{laminar}\,\mathrm{Re}_{\delta^*} \tag{3}$$

(where Re_{δ^*} is the Reynolds number based on displacement thickness) so that the coefficient can now be written in a general form given as

$$\varepsilon_S = \frac{\sqrt{2}\,\mu_{laminar}}{\rho u h}\left(1 + 0.0168\,\mathrm{Re}_{\delta^*}\right). \tag{4}$$

As a test, this formula was exercised for flow over a turbulent flat plate in incompressible flow. It was modified, though, by replacing the displacement thickness with boundary layer thickness. Although this was a rough engineering approximation, comparisons with Dadone's corresponding case [22] revealed that the modified formula produced a surface confinement coefficient quite similar to those used by Dadone et. al.

For the problem at hand, Reference 23 was used to find the boundary layer thickness at the separation point of a cylinder in cross flow and relate it to the cylinder radius. Although it was only possible to find the thickness of a laminar boundary layer, the ratio of measured turbulent and laminar boundary thicknesses in Reference 24 was used to approximate a turbulent layer. In addition, since displacement thickness is a more difficult parameter to obtain than layer thickness, the displacement thickness was replaced with boundary layer thickness, as before. The consequence of all these manipulations was

$$\varepsilon_S = \frac{\sqrt{2}}{\mathrm{Re}_D}\frac{D}{h}\left(1 + 0.1344\sqrt{\mathrm{Re}_D}\right). \tag{5}$$

which casts the coefficient in terms of Reynolds number, cylinder diameter, and cell size.

This equation was applied to the missile airframe but produced a coefficient that was nearly zero. From reviewing the literature, it was judged that this was unworkably small and that a compressibility correction was needed. After some experimentation, it was decided to recast Equation 5 as

$$\varepsilon_S = \frac{\sqrt{2}}{\left(\frac{\mathrm{Re}_D}{100\,M_\infty}\right)}\frac{D}{h}\left(1 + 0.1344\sqrt{\left(\frac{\mathrm{Re}_D}{100\,M_\infty}\right)}\right) \tag{6}$$

for flow scenarios when the freestream Mach number, M_∞, is greater than 1. When employed for the bent nose missile, Equation 6 yielded a coefficient within 4 percent of the default value. Since the calculated coefficient rounded to default value, the default setting was used for the surface confinement calculations that followed.

D. Application with Surface Confinement

To test the veracity of Equation 6, ETA was reapplied to the missile with an 8-degree nose deflection. This airframe was selected because, as is shown in the subsequent section, it produced the greatest disparity between computations and measurement. For these calculations, the default grid settings were used so the downstream boundary was nearly two body lengths from the base, and the other bounds were about one length away. Again, the minimum cell dimensions were set to roughly one one-thousandth (1/1000) of the body length. Nine levels of refinement were specified, resulting in a grid composed of less than 900,000 cells. Computations were then performed for a Mach number of 3.0; roll angles of 0, 45, and 90 degrees; and angles of attack ranging from –10 to +10 degrees. The same grid was used for all these calculations which were made without and with both field and surface confinement. Although there are no upstream control surfaces to generate tip vortices, the deflected nosetip could create a vortex that affects the body flow, especially when it is rolled and at a negative angle of attack. So the field mode was applied as appropriate. Note that the default constants were utilized for both modes of confinement.

III. RESULTS AND DISCUSSION

A. Initial Application

Results for the initial application of ETA to the bent nose configuration are presented in Figures 3 through 6. They are shown in the wind tunnel reference frame and compared with measurements documented in Reference 16. The predictions were performed "blind" without examining any of the wind tunnel data. Yet it is evident from Figures 3 and 4 that the ETA values for normal force and pitching moment agree well with the data for each of the bent nose deflections (each at a roll angle of 0 degrees). In particular, the pitching moment agrees very well especially since it is referenced to the center-of-gravity (a position that amplifies prediction discrepancies). It should also be observed, though, that the pitching moment predictions begin to deviate from the measurements when the sum of the nose deflection and the angle of attack begins to exceed 10 degrees. This behavior is expected since viscous separation is likely to occur above moderate angles of incidence.

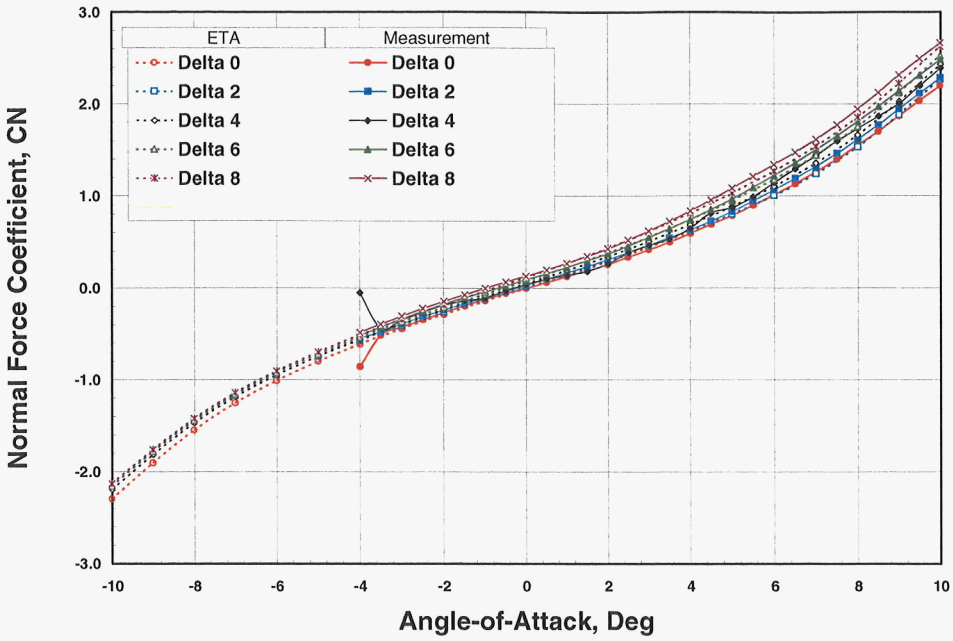

Figure 3. Normal Force Coefficient Versus Angle of Attack for All Bent-Nose Configurations

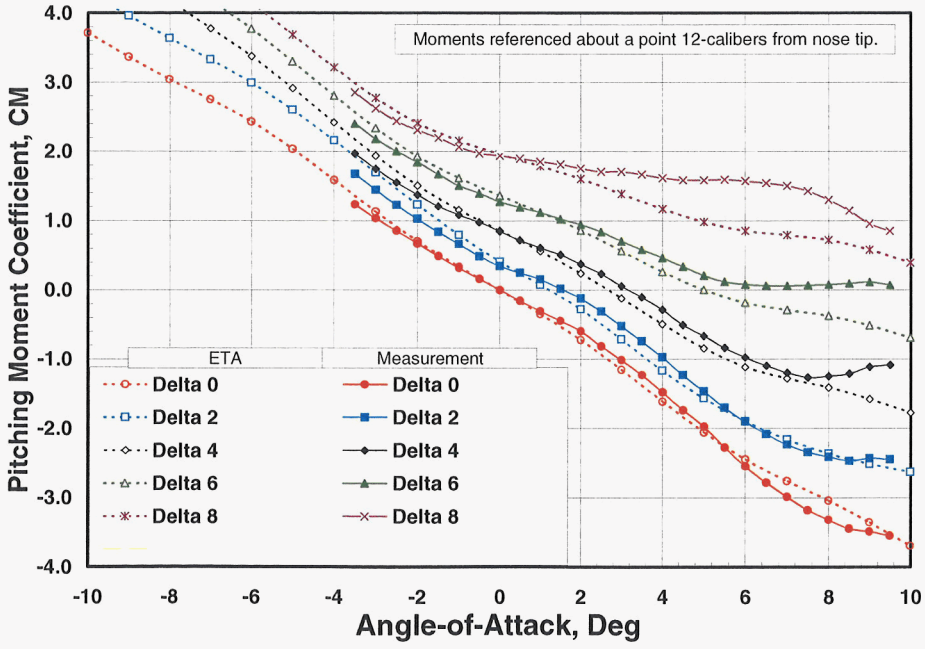

Figure 4. Pitching Moment Coefficient Versus Angle of Attack for All Bent-Nose Configurations

At roll attitudes of 45 and 90 degrees, the normal force and pitching moment curves were nearly coincident with the measurements, so these curves are not shown to save space. Rather, the more demanding comparison of yawing moment is provided in Figures 5 and 6. It can be seen that the agreement with measurement is again quite good up to about 4 degrees angle of attack. Above this, as mentioned before, viscous separation is likely to have occurred.

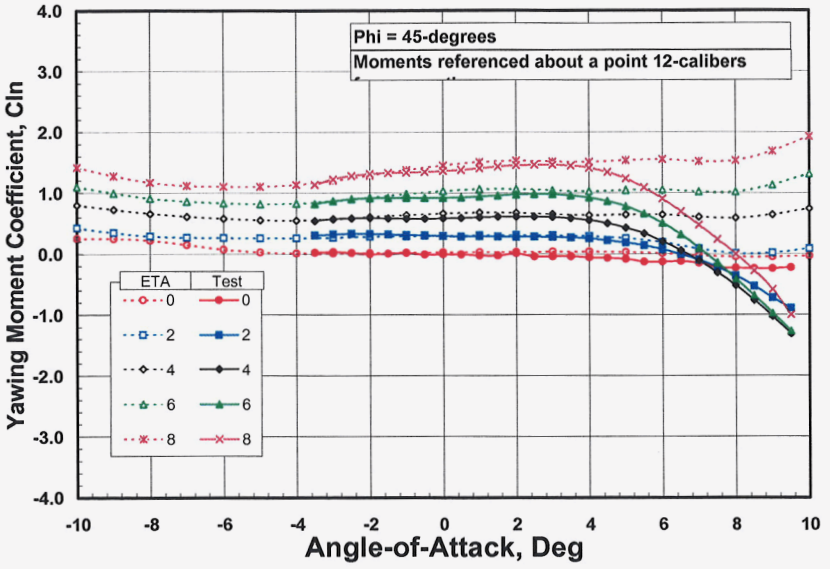

Figure 5. Yawing Moment Coefficient Versus Angle of Attack for All Bent-Nose Configurations at 45-Degree Roll

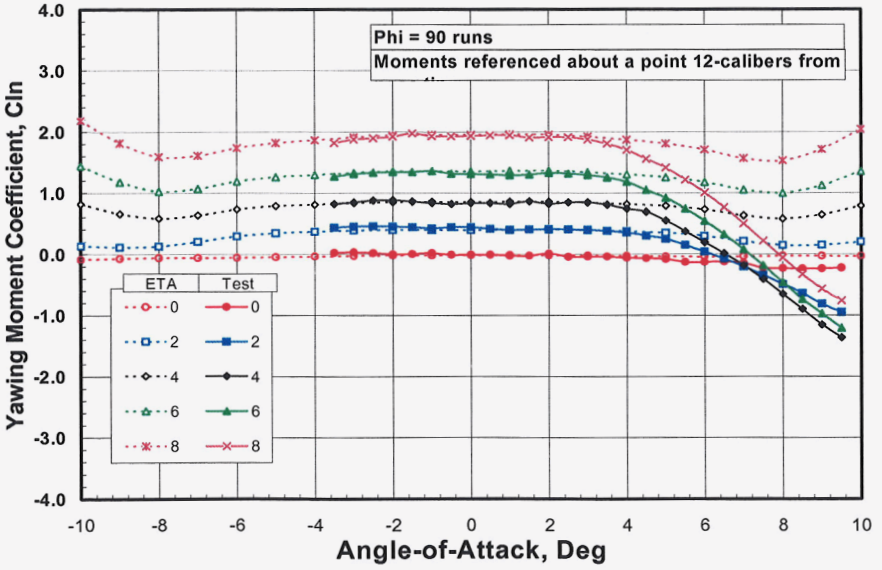

Figure 6. Yawing Moment Coefficient Versus Angle of Attack for All Bent-Nose Configurations at 90-Degree Roll

B. Application with Surface Confinement

Products of the reapplication of ETA with vorticity confinement to the 8 degree bent nose airframe are presented in Figures 7 through 10. In Figure 7, it can be seen that vorticity confinement improves the calculated normal force curve to the point that it is indistinguishable from the wind tunnel data. And in Figure 8, it can be observed that between -4 and 0 degrees of alpha, the technique does not agree with the pitching moment data as well as the strictly Euler results. However, it betters those results by capturing the trend of the measurements between 4 and 10 degrees where flow separation occurs.

The rolled body outcomes for yawing moment are exhibited in Figures 9 and 10. Both of these plots reveal that while the confinement correction produces a slight bias in moment between ±4 degrees, it also begins to capture the correct "roll off" in moment that occurs outside these bounds. Although the favorable comparison with measurement is not as comprehensive as desired, it is clear that the correct kind of flow physics is being approximated. In short, it is evident that the confinement technique is able to account for flow separation on the smooth, cylindrical, missile body whereas the strictly Euler approach is not. This is a significant development in the application of Euler methods. In addition to these observations, it is also evident that even though the surface confinement constant may need some adjusting, the value provided by Equation 6 was appropriate. This lends credence to its validity. It may be that with some further modification, this formula could provide a constant that would enable ETA to match all the yawing moment data shown in these figures.

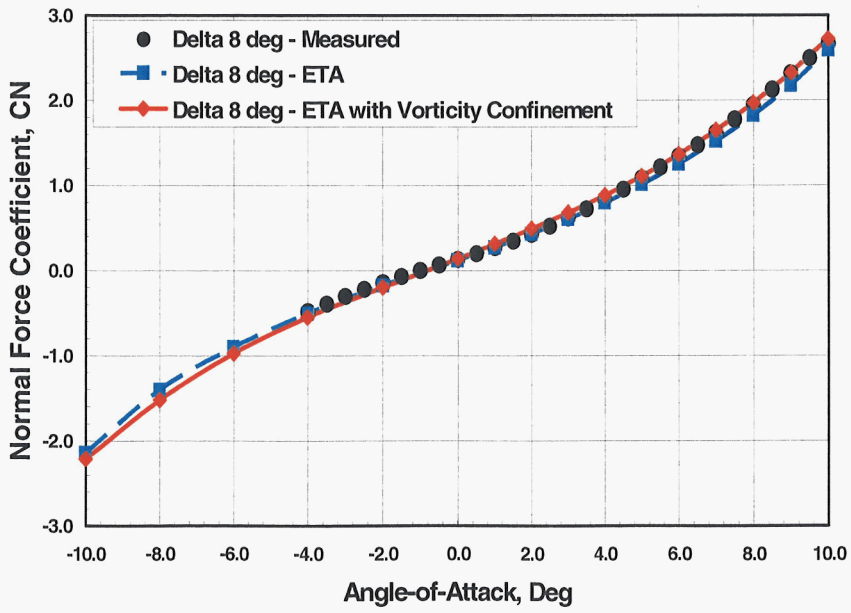

Figure 7. Normal Force Curve for Delta 8 Degree Nose – With/Without Confinement

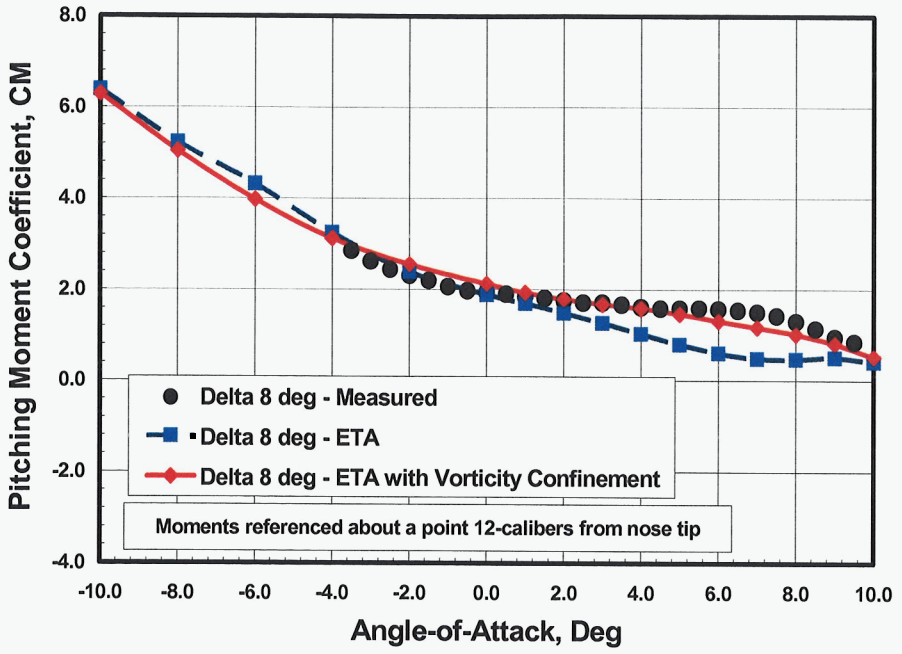

Figure 8. Pitching Moment Force Curve for Delta 8 Degree Nose –with/Without Confinement

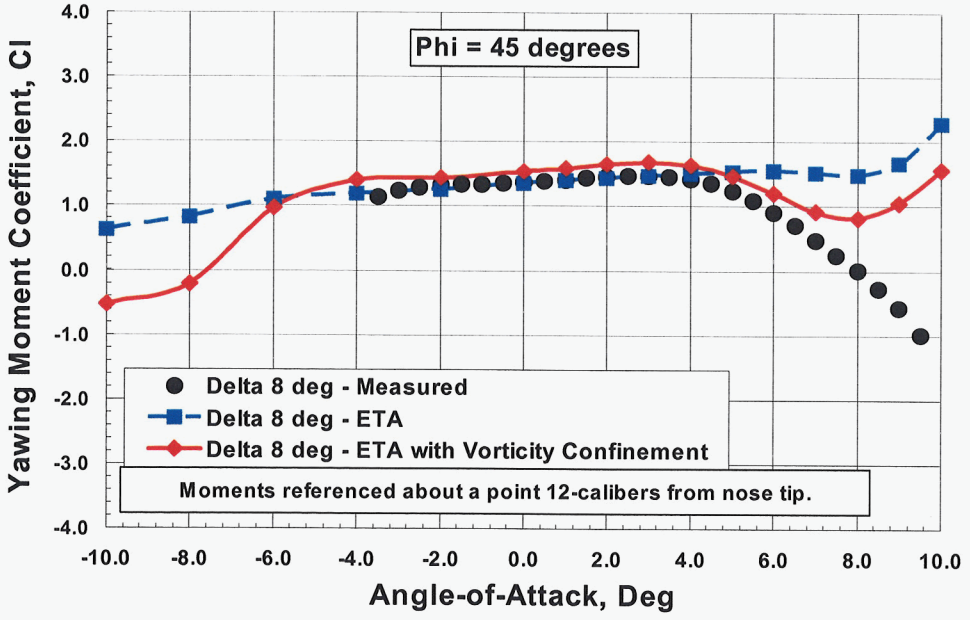

Figure 9. Yawing Moment Curve for Delta 8 Degree Nose at 45-Degree Roll – With/Without Confinement

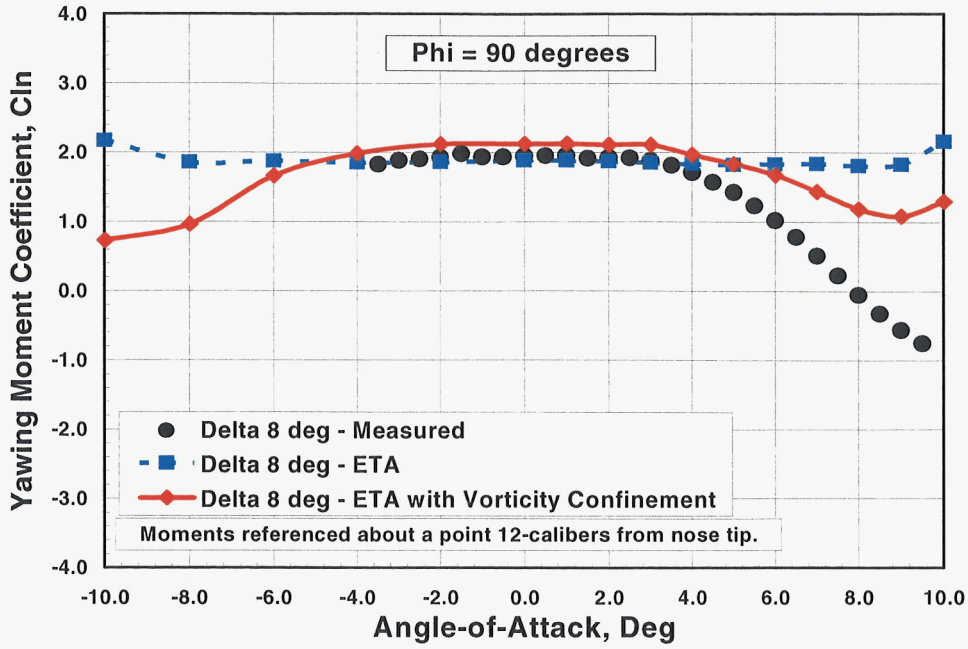

Figure 10. Yawing Moment Curve for Delta 8 Degree Nose at 90-Degree Roll – With/Without Confinement

IV. SUMMARY

It has been shown that the vorticity confinement technique enables an Euler solver to account for the aerodynamic effects of crossflow separation. This was demonstrated in particular for a missile characterized by a high fineness ratio body with a deflected nose at roll angles of 0, 45, and 90 degrees. In addition, a relation has been derived that connects (in general terms) the surface confinement coefficient to physical parameters. When applied to the circular missile body in crossflow, the coefficient produced by the relation was found to yield physically meaningful results. In other words, the ensuing normal force, pitching moment, and yawing moment values were all improved significantly over those produced by strictly Euler computations. And this enhancement was obtained at the low cost of modestly increased computer run time for each Euler flow calculation. Although the improvement was not as comprehensive as desired, it is anticipated that further investigation will yield a more complete form of the equation.

REFERENCES

1. Vaughn, M. E., Jr. and Auman, L. M., "Assessment of Productivity-Oriented CFD Methodology for Designing a Hypervelocity Missile," AIAA Paper 2003-3937, June 2003.

2. Vulelich, S. R., Stoy, S. L., Burns, K. A., Castillo, J. A., and Moore, M. E., "Missile DATCOM Volume I – Final Report," AFWALTR-86-3091, December 1988.

3. Moore, F. G. and Hymer, T. C., "The 2005 Version of the Aeroprediction Code: Part I – Summary of New Theoretical Methodology," January 2004, API Report No.1.

4. Lesieutre, D. J., Love, J. F., and Dillenius, M. F. E., "MISL3 – November 2000 Aerodynamic Analysis for Finned Vehicles with Axisymmetric Bodies," NEAR TR 561, May 2001.

5. Gentry, A. E., Smyth, D. N., and Oliver, W. R., "The Mark IV Supersonic-Hypersonic Arbitrary Body Program, Volume I Users Manual," Technical Report AFFDL-TR-73-159, November 1973.

6. AeroLogic, "Digital Wind Tunnel CMARC Three-Dimensional Low Order Panel Codes," 2000.

7. Magnus, A. E. and Epton, M. A., "PAN AIR – A Computer Program for Predicting Subsonic or Supersonic Linear Potential Flows About Arbitrary Configurations Using A Higher Order Panel Method," Vol. I Theory Document (Version 1.0), NASA CR-3251, 1980.

8. Wardlaw, A. B. and Davis, S. F., "A Second Order Godunov Method for Supersonic Tactical Missiles," NSWC TR 86-506, December 1986.

9. Dietz, W., Fan, M., Steinhoff, J., and Wenren, Y, "Application of Vorticity Confinement to the Prediction of the Flow Over Complex Bodies – A Survey of Recent Results," AIAA Paper 2001-2642, June 2001.

10. Aftosmis, M. J., Berger, M. J., and Melton, J. E., "Robust and Efficient Cartesian Mesh Generation for Component-Based Geometry," AIAA Paper 97-0196, Jan. 1997; and AIAA Journal, Vol. 36, pp, 952-960, June 1998.

11. Melton, J. E, Berger, M. J., and Aftosmis M. J., "3D Applications of a Cartesian Grid Euler Method," AIAA Paper 95-0853, July 1995.

12. Robinson, M. A., "SY-TIGER code Version 5.9 Release Notes & Guide," SYColeman Memorandum, 01 October 2003.

13. Robinson, M. A., "Application of Vorticity Confinement to Inviscid Missile Force and Moment Prediction," AIAA Paper 2004-0717, January 2004.

REFERENCES (CONTINUED)

14. Jameson, A., Schmidt W., and Turkel, E., "Numerical Solutions of the Euler Equations by Finite Volume Methods Using Runge-Kutta Time-Stepping Schemes," AIAA Paper 81-1259, June 1981.

15. Autodesk Inventor Series 5, Getting Started, Autodesk, Inc, December 2001.

16. Roberts, C. B., Auman, L. M., and Landers M. G., "User's Manual for the Compact Kinetic Energy Missile 2000 Aerodynamic Database," U.S. Army Aviation and Missile Command TR-RD-SS-01-29, December 2001.

17. Susen, Y. B. and Hoffman, K. A., "Investigation of Supersonic Jet Exhaust Flow by One- and Two-Equations turbulence Models," AIAA Paper 98-0322, January 1998.

18. Forsythe, J. R., Hoffman, K. A., and Suzen Y. B., "Investigation of Modofied Menter's Two-Equation Turbulence Models for Supersonic Applications," AIAA Paper 99-0873, January 1999.

19. Anderson, D.A., Tannehill, J. C. and Pletcher, R. H., Computational Fluid Mechanics and Heat Transfer, Hemisphere Publishing Corporation, New York, 1984, p 203 and p221.

20. Hinze, J.O., Turbulence, 2nd ed, McGraw-Hill, New York, 1975, p75.

21. Wilcox, Turbulence Modeling for CFD, 2nd ed, DCW Industries, Inc., La Canada, California, 2004, pp 74-75.

22. Dadone, A., Hu, G., and Grossman, B., "Towards a Better Understanding of Vorticity Confinement in Compressible Flow," AIAA Paper 2001-2639, June 2001.

23. Schlichting, Boundary Layer Theory, 6th ed., McGraw-Hill, New York, 1968, p202.

24. Schubauer, G. B., and Klebanoff, P. S., "Contributions on the Mechanics of Boundary-Layer Transition," NACA Report 1289, 1956.

INITIAL DISTRIBUTION LIST

		Copies
Weapon Systems Technology Information Analysis Center 1901 N. Beauregard Street, Suite 400 Alexandria, VA 22311-1720	Mr. Perry Onderdonk ponderdonk@alionscience.com	Electronic
Defense Technical Information Center 8725 John J. Kingman Rd., Suite 0944 Fort Belvoir, VA 22060-6218	Jack Rike jrike@dtic.mil	Electronic
AMSRD-AMR		Electronic
AMSRD-AMR-CS-IC		Electronic
AMSRD-AMR-SS,	Mr. Gregory B. Tackett Gregory.Tackett@us.army.mil	Electronic
AMSRD-AMR-SS-AT,	Mr. Lamar M. Auman lamar.auman@us.army.mil	Electronic
	Mr. Milton E. Vaughn, Jr. Ed.Vaughn@us.army.mil	Electronic
AMSRD-L-G-I,	Ms. Anne Lanteigne anne.lanteigne@us.army.mil	Electronic